PCCP

Accepted Manuscript

ROYAL SOCIETY OF CHEMISTRY

www.rsc.org/pccp

Journal Name

RSCPublishing

ARTICLE

Geometries, stabilities and fragmental channels of neutral and charged sulfur clusters: S_n^Q (n = 3-20, Q = 0, ±1)

Cite this: DOI: 10.1039/xoxxoooooox

Received ooth January 2015,
Accepted ooth January 2015

DOI: 10.1039/xoxxoooooox

www.rsc.org/

Yuanyuan Jin,[a] George Maroulis,[b] Xiaoyu Kuang,[a*] Liping Ding,[a] Cheng Lu,[c*] Jingjing Wang,[a] Jian Lv,[d,e*] Chuanzhao Zhang[a] and Meng Ju[a]

We have performed unbiased searches for the global minimum structures of neutral and charged sulfur clusters S_n^Q (n = 3-20, Q = 0, ±1) relying on the CALYPSO structure searching method combined with density functional theory geometric optimization. Very accurate *ab initio* calculations are used to determine relative stabilities and energy ranking among competing low-lying isomers of the neutral and charged sulfur clusters obtained from the structure search. Harmonic vibrational analysis is also undertaken to assure that the optimized geometries are true minimum. It is shown that the most of equilibrium geometries of sulfur clusters are closed three-dimensional (3D) helical rings, which is in agreement with the experimental observations. The binding energies, second-order energy difference, highest occupied–lowest unoccupied molecular orbital (HOMO–LUMO) gaps of the considered species are calculated and analyzed systematically. Additionally, the fragmentation channels are determined and the results indicate that $S_n^Q \rightarrow S_2 + S_{n-2}^Q$ channel is a route that the small clusters (n = 3-10) favor, while the larger species (n = 13-20) prefer the $S_n^Q \rightarrow S_8 + S_{n-8}^Q$ channel.

1. Introduction

Sulfur is an essential element for all life. It is an important part of many enzymes and in antioxidant molecules like glutathione and thioredoxin.[1,2] Bonded sulfur is a component of all proteins, such as the amino acids cysteine and methionine.[3] Disulfide bonds are largely responsible for the mechanical strength and insolubility of the protein keratin, found in outer skin, hair, and feathers.[4] Chemically, sulfur can react as either an oxidant or a reducing agent. It oxidizes most metals and several nonmetals, including carbon, which leads to its formal negative charge in most organosulfur compounds, but it reduces several strong oxidants, such as oxygen and fluorine.[5,6]

Sulfur occupies a unique position in the periodic table with regard to one of the largest numbers of solid allotropes. At present, about 30 crystalline allotropes are known. Experimental work[7-13] reveal that there exist a large number of conformations with open chain-like, closed cyclic or puckered chair/boat forms in the solid, liquid and vapor phases of the sulfur clusters and the homocyclic ring structures have received great attention from both the experimental and theoretical points of view. In order to obtain a better understanding of the properties of sulfur microparticles, it is of both fundamental and practical interest to investigate the structures and properties of small-to-medium sized clusters. Extensive studies have been performed on the geometric structures of low-energy sulfur clusters, relative stabilities along with a search for their growth pattern. Hohl et al. investigated the ground state geometries of neutral sulfur clusters up to n = 13 using a parameter free density functional method, combined with molecular dynamics and simulated annealing techniques.[14] Based on the *ab initio* quantum chemical calculations, Raghavachari et al. explored the geometric structures and relative stabilities of small sulfur clusters (S_2-S_{12}) by considering the effects of polarization functions and electron correlation.[15] In order to elucidate the growth behavior of the sulfur clusters, Millefiori and Alparone performed extensive theoretical calculations of the structures and polarizabilities of S_n clusters (n = 2-12), relying on density functional theory within the B3LYP approximation and conventional *ab initio* Hartree-Fock (HF) and coupled cluster with single and double and perturbative triple excitations (CCSD (T)) methods.[16] Using density functional calculations, Jones and Ballone investigated the rings isomers of sulfur clusters with up to 18 atoms and for chains with up to ten atoms.[17]

Although the structures of small sulfur cluster have been extensively studied and enormous progress has been made, the true lowest-energy isomers of the other sulfur clusters, for example the medium sized S_n clusters, are still debatable. The main reasons may be as follows: (i) The procedure used in the case of small clusters is not practical for the medium sized clusters. (ii) The predicted global minima are subtle sensitivity for the selected density functional theory, or the molecular-orbital level in the *ab initio* calculations. Moreover, the determination of the true global minimum structure is also a challenging problem, because of much increased complexity of the potential surface as well as the exponential increase of the lowest-energy structures with increasing number of atoms in the cluster.

In order to systematically study the structural evolution and electronic properties of sulfur clusters, we present comprehensive structure searches to explore the global minimum geometric structures of small and medium-sized neutral but also charged sulfur clusters in the size range of n = 3-20, by combining our developed CALYPSO method with density functional theory calculations. Our first goal of this work is to gain a fundamental understanding of the ground state geometric structures of medium-sized sulfur clusters. The second one is to reexamine a number of neutral and charged low-energy isomers of small sulfur clusters that have been reported previously by experiments or density functional calculations. Thirdly, we are also motivated to explore the physical mechanism of the growth behaviors of medium-sized sulfur clusters and provide relevant information for further theoretical and experimental studies.

The rest of the article is organized as follows. A brief description of the computational details is presented in Sec. 2. Section 3 presents the results and their discussion and is subdivided into five subsections. In Sec. 3.1 we provide a brief overview of the ground state geometries of the neutral and charged S_n^Q (n = 3-20, Q = 0, ±1) clusters. Details about the relative stabilities of the global minimum structures are provided in Sec. 3.2. The fragmentation behaviors of small and medium sized sulfur clusters are discussed in Sec. 3.3. The ionization energy and electron affinity potential calculations are described in Sec. 3.4. Finally, the main conclusions of the article are summarized in Sec. 4.

2. Computational details

Our approach involves global minimization of energy surfaces, merging *ab initio* total energy calculations via CALYPSO cluster prediction based on the particle swarm optimization algorithm in the CALYPSO code.[18-20] The significant feature of this method is the capability of predicting the most stable structure depending only on the knowledge of the chemical composition. It has been successful in correctly predicting structures for various systems.[20-22] Structure predictions of the neutral and charged sulfur clusters are performed for cluster size n = 3-20. Each generation contains 30 structures, 60% of which are generated by PSO. The others are new and will be generated randomly. We followed 50 generations to achieve the converged structures.

The low-lying candidate structures of the global minimum for each size are further optimized using all-electron density functional theory within the B3PW91[23-25] functional of generalized gradient approximation, as implemented in the Gaussian 09 package.[26] The basis set 6-311+G* is selected for the determination of the lowest-energy structures of sulfur clusters. In detail, the validity of this method is illustrated in the Electronic Supplementary Information (ESI). Then a more flexible aug-cc-pVDZ basis set is also employed to calculate the single point energy of these clusters. The convergence thresholds of the maximum force, root-mean-square (RMS) force, maximum displacement of atoms, and RMS displacement are set to 0.00045, 0.0003, 0.0018, and 0.0012 a.u., respectively. The effect of the spin multiplicity is also taken into account in the geometric optimization procedure. Meanwhile, the vibrational frequency calculations are performed at the same level theory to assure the nature of the stationary points.

3. Results and discussion

3.1 Geometrical structures

The global minimum geometries of S_n^Q (n = 3-20, Q = 0, ±1) clusters are shown in Figs. 1-3. The other low-lying isomers of sulfur clusters together with their relative energies are shown in Figs. S2-S4 in the ESI. All the equilibrium structures are searched by CALYPSO method and optimized at the B3PW91/6-311+G* level of theory. All the previously reported structures, experimentally and theoretically, were successfully reproduced in our current structure searches. The

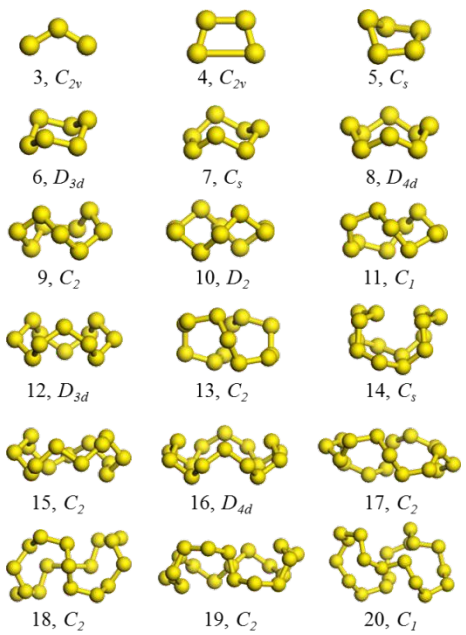

Fig. 1. Lowest-energy structures of S_n (n = 3-20) clusters.

calculated vibrational frequencies and the bond lengths are collected in Tables S6-S8 and Tables S9-S11, respectively. Their positive frequencies show that the calculated structures correspond to true minima. From Figs. 1-3, only the ground-state structures of S_3^Q and S_4^Q (Q = 0, ±1) are exactly planar, while the equilibrium structures of the neutral and charged sulfur clusters (n > 4) are non-planar. The ground-state neutral S_n (n = 3-20) clusters (Fig. 1) possess substantially high point symmetry except for the case of S_{11} and S_{20}: S_3 and S_4 are of C_{2v} symmetry; S_6 and S_{12} are of D_{3d} symmetry; S_8 and S_{16} are of D_{4d} symmetry; S_5, S_7 and S_{14} are of C_s symmetry; S_{10} possesses D_2 symmetry; others belong to the C_2 symmetry. All S_n clusters with n > 4 possess closed three-dimensional ring-shaped structures. The ground-state geometries of small S_5-S_8 are excellent agreement with the results of and Dixon et al..[27] However, the C_2 symmetry S_{11} cluster (Fig. S2), previously experimentally studied by Steudel et al.[28], is rechecked in this work. Our results show that this structure is ~0.03 eV higher than the newly proposed ground-state structure with C_1 symmetry (Fig. 1). In addition, the equilibrium ring-type geometries of neutral S_{14}-S_{20} are comprehensively predicted. We found that the symmetries of S_7 (C_s) and S_8 (D_{4d}) are identical to those of the S_{14} and S_{16}, respectively. The rest of neutral sulfur clusters are characterized by C_2 symmetry with the notable exception of S_{20}. In fact, the structure of S_{20} with C_2 symmetry (Fig. S2) is only 0.09 eV higher in energy than the ground-state structure (Fig. 1).

The global minimum structures of anionic S_n^- (n = 3-20) clusters (Fig. 2) are essentially different from those of the neutral species. The structures of S_3^- and S_4^- are in accord with the results of Chen et al.,[29] although the S_4^- structure is different from that reported by Hunsicker et al. and Zakrzewski et al..[10,30] In addition, Hunsicker et al.[10] and Zakrzewski et al.[30] have reported a C_s symmetry S_5^- (Fig. S3) as the lowest-energy structure, ~0.02 eV higher than our expected S_5^- of C_2 symmetry (Fig. 2). The equilibrium geometries of S_6^- and S_7^- are in good agreement with the results of Hunsicker et al. and Chen et al..[10,29] For clusters of size n > 7, Chen et al. claimed that most ring-shaped structures have imaginary frequencies whereas the chain-shaped structures are characterized by real frequencies.[29] However, the ring-shaped C_2 symmetry S_8^- is found to be the ground-state structure in this study. The D_2 symmetry S_8^- reported by Hunsicker et al. is shown to be a transition state.[10] The ground-state structure of S_9^- is also of ring-type with C_2 symmetry. Apart from S_{18}^-, which is no longer closed helical ring but a combination of ring and chain form, anionic sulfur clusters from S_{10}^- to S_{20}^- are all closed 3D helical ring-shaped. The energy of ground-state S_{18}^- (Fig. 2) is lower than the helical ring S_{18}^- with C_2 symmetry (Fig. S3) by ~0.24 eV.

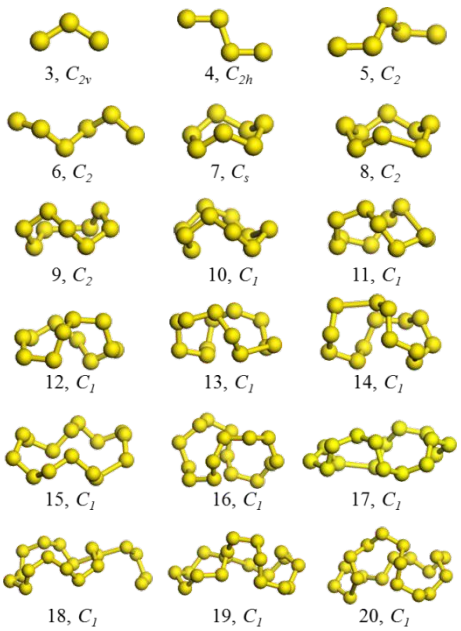

Fig. 2. Lowest-energy structures of S_n^- (n = 3-20) clusters.

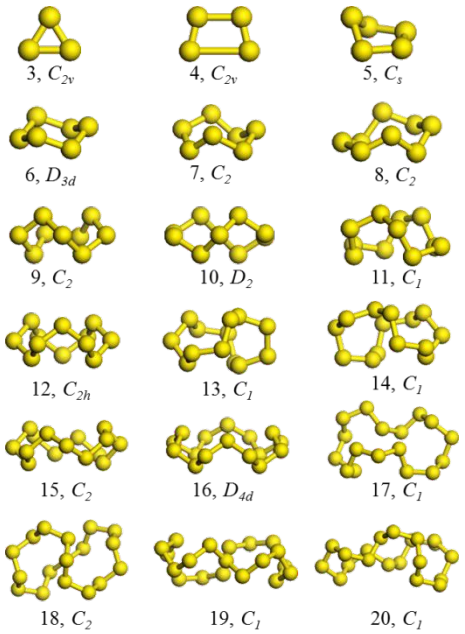

Fig. 3. Lowest-energy structures of S_n^+ (n = 3-20) clusters.

The symmetries of global minimum sulfur cations (Fig. 3) are mostly identical to the respective neutral species, with the exception of n = 7, 13, 14, 17 and 20. The structures of S_3^+-S_7^+ and S_{10}^+ are in agreement with those reported by Chen et al..[31] Unfortunately, there are no available experimental data for comparison. The C_2 symmetry S_8^+ cluster is similar to the respective neutral state but with a slightly distorted geometry. The lowest-energy structure of S_{12}^+ is found to be of C_{2h} symmetry. However, the D_{3d} symmetry S_{12}^+ structure proposed by Chen et al.[31] is not a true local minimum structure, as shown by the results of our vibrational frequency analysis. The equilibrium structures of S_{15}^+, S_{16}^+, S_{18}^+ and S_{19}^+ display the same closed helical form as their neutral state,

indicating that the loss of an electron has truly a little effect on the geometric structures of the resulting cations.

3.2 Relative stability

Tables S12-S14 in the ESI give the energetic characteristics of the lowest-energy structures for S_n^Q (n = 3-20, Q = 0, ±1) clusters. Stability of a cluster might be judged through its binding energy (E_b) per atom, for neutral, anionic and cationic sulfur clusters, which can be defined as:

$$E_b(S_n) = \left[nE(S) - E(S_n)\right] / n \quad (2)$$

$$E_b(S_n^-) = \left[(n-1)E(S) + E(S^-) - E(S_n^-)\right] / n \quad (3)$$

$$E_b(S_n^+) = \left[(n-1)E(S) + E(S^+) - E(S_n^+)\right] / n \quad (4)$$

where E is the total energy of the cluster. The E_b quantities as functions of cluster size are given in Fig. 4 (a). Fig. 4 (a) shows that the E_b values of cationic S_n^+ are always much higher than their neutral and anionic states. It is also easily observed that for neutral and anionic sulfur species, the binding energies increase monotonically with cluster size growing and reach maxima at n = 8, indicating that the S_8 and S_8^- are relatively more stable in the region of n = 3-8. A similar scenario has been reported by Jones and Ballone.[17] Then the binding energies become almost stable when n > 8. The trend characterizing of the neutral E_b curve in the cluster size S_3-S_{12} is in obvious agreement with the theoretical results of Millefiori and Alparone calculated at the B3LYP level of theory.[16] As for cationic S_n^+ clusters, a maximum of 2.86 eV is found at n = 5, which indicates that S_5^+ is the relatively most stable cation.

The second-order difference of energy (Δ^2E) is a sensitive quality, reflecting the relative stability of clusters. For the S_n^Q (n = 3-20, Q = 0, ±1) clusters, the Δ^2E values are calculated by

$$\Delta^2E(S_n) = E(S_{n-1}) + E(S_{n+1}) - 2E(S_n) \quad (5)$$

$$\Delta^2E(S_n^-) = E(S_{n-1}^-) + E(S_{n+1}^-) - 2E(S_n^-) \quad (6)$$

$$\Delta^2E(S_n^+) = E(S_{n-1}^+) + E(S_{n+1}^+) - 2E(S_n^+) \quad (7)$$

The Δ^2E as functions of size for S_n^Q (n = 3-20, Q = 0, ±1) clusters are shown in Fig. 4 (b). From Fig. 4 (b), it reveals obvious odd-even oscillation in the range of n = 5-17 for neutral clusters S_n and several conspicuous maxima are found at n = 6, 8, 10, 12, 14 and 16, a fact suggesting that the respective even size clusters S_n are more stable compared to their odd counterparts. It is also worth noticing that the Δ^2E curves of neutral and anionic clusters present the same oscillation in the range of n = 7-12, while present opposite trends from n = 13-19. Moreover, the maximum peaks of Δ^2E curve for anionic clusters imply that $S_{8,15,17,19}^-$ have strong relatively stability. In the case of cationic clusters, a similar trend of Δ^2E curves for neutral and cationic clusters is present in the range n = 9-18. Furthermore, the more relatively stable cations are S_n^+ with n =5, 7, 10, 12, 14, and 16, due to their higher Δ^2E values.

The energy gap (E_{gap}) between the highest occupied molecular orbital and the lowest unoccupied molecular orbital reflects the ability of electron to jump from occupied orbital to unoccupied orbital. A large HOMO–LUMO gap is a signature of the chemical stability as the cluster wants to neither donate nor receive charge.[32] The calculated E_{gap} values of ground-state S_n^Q (n = 3-20, Q = 0, ±1) clusters are summarized in Table S10-S12 in the ESI. For clarity, the E_{gap} values as functions of cluster size are plotted in Fig. 4 (c). Comparing the E_{gap} values of neutral, anionic and cationic sulfur clusters, we can see that the E_{gap} values of neutral S_n are always the highest, signifying that neutral S_n clusters have the relatively stronger chemical stability. In addition, the most stable structure can be assigned to S_8 cluster due to local maximum E_{gap} = 4.73 eV is found at n = 8. The neutral S_{12} also exhibits relatively large E_{gap} values. In the case of anionic clusters, we find that after attaching an electron, the relative stability of S_5^-

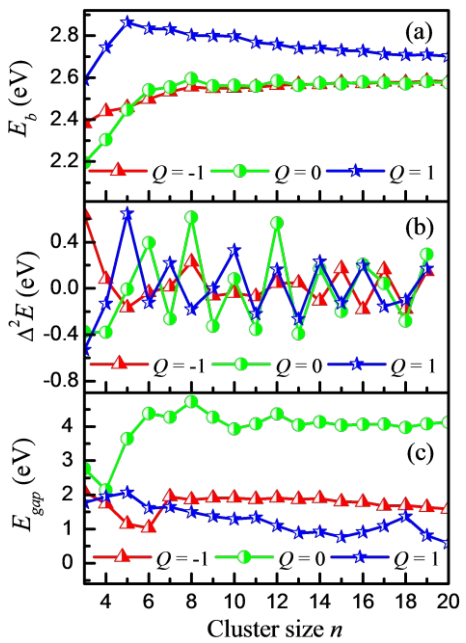

Fig. 4. Binding energies, second energy differences and HOMO–LUMO gaps of sulfur clusters S_n^Q (n = 3-20, Q = 0, ±1) as functions of cluster size n.

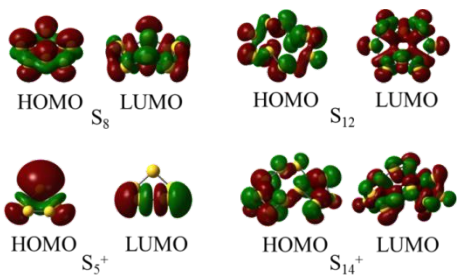

Fig. 5. Highest occupied (HOMO) and lowest unoccupied molecular orbital (LUMO) for magic neutral S_8 and S_{12}, as well as cationic S_5^+, and S_{14}^+ clusters.

and S_6^- undergo changes, namely, S_5^- and S_6^- becomes relative unstable. In addition, the HOMO–LUMO gaps of sulfur anions become almost stable in the cluster size of $n > 7$. From the E_{gap} curve of cationic clusters in Fig. 4 (c), the local maxima of cationic clusters occur at n = 5, 14 and 18. Moreover, considering the theoretical Δ^2E analysis, it can be concluded that the magic sulfur clusters are neutral S_8 and S_{12}, as well as cationic S_5^+ and S_{14}^+. Fig. 5 displays the HOMO and LUMO pictures of these magic sulfur clusters. These MOs are all of S 3*p* characters. The HOMO of neutral S_8 (Fig. 5) is specially a π-bonding orbital, whereas other magic clusters possess σ-type bond.

In order to further check the structural feature of sulfur cluster, we have calculated their vibrational spectra. For the magic number S_8, the infrared (IR) and Raman spectra are displayed in Fig. 6 (a) and (b), respectively. The insets show the direction vectors of S_8 for the frequency with the highest infrared intensity or Raman activity. The two spectra can provide spectroscopic fingerprint to assist experimentalists to distinguish between different species and different isomers. From the insets in Fig. 6 (a) and (b), it can be easily found that due to the high D_{4d} symmetry, all S atoms contribute to the highest peaks of infrared spectrum and Raman activity and the direction vectors are pointing to the outside in Fig. 6 (a) and pointing to the inside in Fig. 6 (b). As displayed in Fig. 6 (a), there are three conspicuous peaks. The highest intense peak of infrared spectra is 34.3 km/mol at frequency 191.1 cm^{-1}. The second and third degenerate IR intense peaks occur at frequency 239.0 cm^{-1} and frequency 454.8 cm^{-1}. For the Raman spectra, four strong vibration peaks are found in Fig. 6 (b). Raman activity mainly corresponds to the breathing modes and in these modes all the ions in clusters having high symmetry move together. The highest Raman activity is 3.1 $Å^4$/amu at frequency 213.9 cm^{-1}.

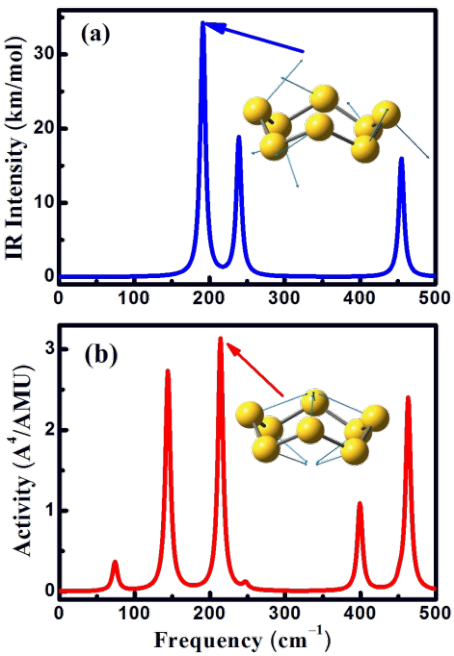

Fig. 6. The gaussian broadened infrared intensities and Raman activities of neutral S_8 cluster. Insets show the frequency modes corresponding to the highest intensity or activity.

3.3 Fragmentation channels

As known, fragmentation processes may involve dissociation barriers. The fragmentation energies E_f (the total energy differences between reactants and products) for neutral and charged sulfur clusters can be expressed as

$$E_f(S_n) = E(S_p) + E(S_{n-p}) - E(S_n), \quad p = 1\text{-}19. \tag{8}$$

$$E_f(S_n^-) = E(S_p) + E(S_{n-p}^-) - E(S_n^-), \quad p = 1\text{-}19. \tag{9}$$

$$E_f(S_n^+) = E(S_p) + E(S_{n-p}^+) - E(S_n^+), \quad p = 1\text{-}19. \tag{10}$$

In general, if E_f is negative for a fragmentation channel, the parent cluster is unstable against that process, and it may dissociate spontaneously by releasing an amount of energy E_f. On the other hand, a positive E_f shows that the parent is stable against that channel, and one must supply energy for the realization of that fragmentation. The most probable channels are those yielding the lowest E_f.[33]

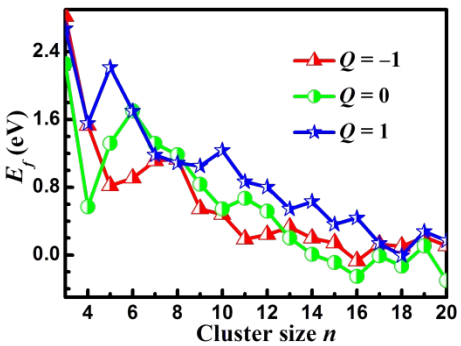

Fig. 7. The fragmentation energies of the easiest fragmentation channels for sulfur clusters S_n^Q (n = 3-20, Q = 0, ±1).

The calculated fragmentation energy values of the most probable fragmentation channels for neutral, anionic and cationic sulfur clusters are summarized in Table 1. From Table 1, it is evident that the E_f values of neutral S_{15}-S_{18} and S_{20}, anionic S_{16}^- and cationic S_{18}^+ are negative, which indicates that the parent clusters may be unstable against the most probable channel. As an example, the most unstable neutral S_{20} would dissociate to S_8 and S_{12} by releasing 0.30 eV energy. Table 1 also show that S_2 and S_8 are repeated most often in fragmentation products, meaning that when sulfur clusters decompose into S_2 and S_8, their fragmentation energies are smaller compared to other channels. In addition, the $S_n^Q \rightarrow S_2 + S_{n-2}^Q$ channel is a route favored by the smaller clusters (n = 3-10), while the larger S_n^Q (n = 13-20) clusters prefer the $S_n^Q \rightarrow S_8 + S_{n-8}^Q$ channel.

Table 1. The fragmentation energies (E_f) of the easiest fragmentation channels for S_n^Q (n = 3-20, Q = 0, ±1) clusters.

Clusters	S_p+S_{n-p}	E_f (eV)	Clusters	$S_p+S_{n-p}^-$	E_f (eV)	Clusters	$S_p+S_{n-p}^+$	E_f (eV)
S_3	S_2+S	2.26	S_3^-	S_2+S^-	2.82	S_3^+	$S+S_2^+$	2.67
S_4	S_2+S_2	0.57	S_4^-	$S_2+S_2^-$	1.53	S_4^+	$S_2+S_2^+$	1.55
S_5	S_2+S_3	1.32	S_5^-	$S_2+S_3^-$	0.82	S_5^+	$S_2+S_3^+$	2.21
S_6	S_2+S_4	1.70	S_6^-	$S_2+S_4^-$	0.91	S_6^+	$S_2+S_4^+$	1.70
S_7	S_2+S_5	1.32	S_7^-	$S_2+S_5^-$	1.11	S_7^+	$S_2+S_5^+$	1.18
S_8	S_2+S_6	1.19	S_8^-	$S_2+S_6^-$	1.13	S_8^+	$S_2+S_6^+$	1.09
S_9	S_2+S_7	0.84	S_9^-	$S_6+S_3^-$	0.55	S_9^+	$S_2+S_7^+$	1.05
S_{10}	S_2+S_8	0.55	S_{10}^-	$S_7+S_3^-$	0.48	S_{10}^+	$S_2+S_8^+$	1.23
S_{11}	S_6+S_5	0.67	S_{11}^-	$S_8+S_3^-$	0.19	S_{11}^+	$S_6+S_5^+$	0.87
S_{12}	S_6+S_6	0.52	S_{12}^-	$S_8+S_4^-$	0.24	S_{12}^+	$S_2+S_{10}^+$	0.80
S_{13}	S_6+S_7	0.20	S_{13}^-	$S_8+S_5^-$	0.33	S_{13}^+	$S_8+S_5^+$	0.54
S_{14}	S_6+S_8	0.01	S_{14}^-	$S_8+S_6^-$	0.20	S_{14}^+	$S_8+S_6^+$	0.63
S_{15}	S_8+S_7	–0.09	S_{15}^-	$S_8+S_7^-$	0.14	S_{15}^+	$S_8+S_7^+$	0.36
S_{16}	S_8+S_8	–0.25	S_{16}^-	$S_8+S_8^-$	–0.07	S_{16}^+	$S_8+S_8^+$	0.44
S_{17}	S_8+S_9	–0.01	S_{17}^-	$S_8+S_9^-$	0.13	S_{17}^+	$S_8+S_9^+$	0.14
S_{18}	S_8+S_{10}	–0.13	S_{18}^-	$S_8+S_{10}^-$	0.10	S_{18}^+	$S_8+S_{10}^+$	–0.01
S_{19}	S_8+S_{11}	0.11	S_{19}^-	$S_8+S_{11}^-$	0.21	S_{19}^+	$S_8+S_{11}^+$	0.28
S_{20}	S_8+S_{12}	–0.30	S_{20}^-	$S_8+S_{12}^-$	0.11	S_{20}^+	$S_8+S_{12}^+$	0.17

To clarify this point, the fragmentation energies of the most favorable channels as function of cluster size are plotted in Fig. 7. From Fig. 7, the evidently higher relative stability associated with an energy maximum is observed for S_3, S_6 and S_{19} for neutrals, as well as S_3^-, S_8^- and S_{13}^- for anions, and S_3^+, S_5^+, S_{10}^+, S_{14}^+, S_{16}^+ and S_{19}^+ for cations. In addition, for neutral and cationic clusters, the fragmentation energy curve displays obvious overall drop behavior in the range of $n > 6$, whereas the overall decline trend happens for $n > 8$ for anionic clusters. This phenomenon suggests that the clusters with larger size are relatively more unstable and easier dissociated.

3.4 Ionization potentials and electron affinity

The ionization potential (IP) and electron affinity potential (EA) are two significant characteristics of the electronic properties for clusters. For sulfur clusters, they are calculated by

$$\mathrm{IP} = E(\mathrm{S}_n^+) - E(\mathrm{S}_n) \quad (11)$$

$$\mathrm{EA} = E(\mathrm{S}_n) - E(\mathrm{S}_n^-) \quad (12)$$

where $E(S_n)$ is the total energy of ground state neutral cluster. In the Eq. (11), when $E(S_n^+)$ is the total energy of optimized cationic cluster, the IP is adiabatic (AIP); if $E(S_n^+)$ represents the total energy of unoptimized cation at optimized neutral cluster, the IP become vertical (VIP). In the Eq. (12), the EA is adiabatic (AEA) when $E(S_n^-)$ is the total energy of ground state anionic cluster and it becomes vertical (VEA) if $E(S_n^-)$ is the total energy of unoptimized anion at optimized neutral sulfur. Moreover, the vertical detachment energy (VDE) can also be evaluated from Eq. (12) if $E(S_n)$ represents the total energy of the unoptimized neutral cluster at the equilibrium anion and $E(S_n^-)$ is the total energy of ground state anion. The calculated results for the AIP and VIP, VEA, AEA and VDE are summarized in Table 2 along with available experimental and theoretical data. Unfortunately, only small sulfur clusters (n = 3-12) have been determined experimentally. No experimental values available for larger size clusters. We observe that our results of AIP, VIP, VEA and AEA are satisfactory. Most of the VDE values deviate by ~0.5 eV from the experimental results.[10] Furthermore, the cluster size dependences of VIP and AIP for sulfur clusters are shown in Fig. 8. We notice that the two curves show a similar oscillation tendency, which means that the lowest-energy structures of neutral S_n clusters are similar to cationic S_n^+ clusters. In addition, the VIP and AIP curves exhibit the same local maximum at n = 6, 8 and 12, a fact explaining the enhanced stability of S_6, S_8 and S_{12}.

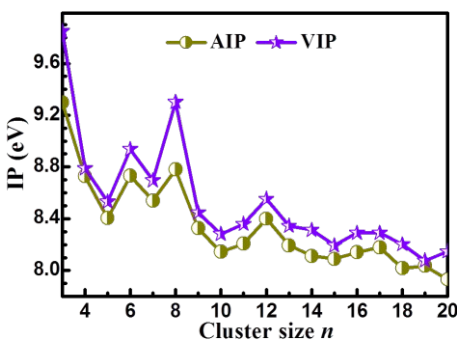

Fig. 8. The ionization potential of S_n^Q (n = 3-20, Q = 0, ±1) clusters as functions of the cluster size n.

Table 2. The calculated AIP and VIP, VEA, AEA and VDE values for sulfur clusters, together with available experimental and theoretical data for comparison.

	AIP (eV)		VIP (eV)		VEA (eV)	AEA (eV)		VDE (eV)	
	Theo.	Exp.	Theo.	Exp.	Theo.	Theo.	Exp.	Theo.	Exp.
S_3	9.39, 9.53[a]	9.68[b]	9.88, 9.80[a]		2.59, 2.13[a]	2.76, 2.38[a]	2.40[c]	2.93, 2.64[c]	2.50[c]
S_4	8.75, 8.56[a]		8.86, 8.68[a]		2.61, 2.27[a]	2.77, 2.46[a]	2.38[c]	2.93, 2.49[c]	2.42[c]
S_5	8.55, 8.20[a]	8.60[b]	8.68, 8.22[a]		1.03, 2.10[a]	2.38, 2.23[a]		3.74, 2.85[c]	2.97[c]
S_6	8.82	9.00[b]	9.10	9.0[d]	1.04	2.13	1.68[c]	4.01, 3.55[c]	3.35[c]
S_7	8.74	8.67[b]	8.88		1.01	2.18		3.16, 3.52[c]	3.38[c]
S_8	8.99	9.04[b]	9.48	9.04[d]	1.25	2.02		3.06, 3.62[c]	3.87[c]
S_9	8.57		8.66		1.12	2.23		3.24, 3.68[c]	3.90[c]
S_{10}	8.37		8.50		1.49	2.19		3.34,	3.90[c]
S_{11}	8.44		8.57		1.49	2.25		3.29,	3.75[c]
S_{12}	8.59		8.75		1.54	2.03		3.39	
S_{13}	8.44		8.56		1.55	2.30		3.34	
S_{14}	8.40		8.52		1.64	2.21		3.31	
S_{15}	8.31		8.38		1.69	2.44		3.41	
S_{16}	8.35		8.47		1.96	2.23		3.40	
S_{17}	8.35		8.55		1.82	2.37		3.44	
S_{18}	8.19		8.40		1.97	2.41		3.91	
S_{19}	8.23		8.28		1.77	2.35		3.54	
S_{20}	8.17		8.36		1.83	2.44		3.42	

[a] Refer. 30. [b] Refer. 34. [c] Refer. 10. [d] Refer. 35

4. Conclusions

The equilibrium structures of S_n^Q (n = 3-20, Q = 0, ±1) clusters have been obtained by using the CALYPSO search combined with an *ab intio* DFT method. The results are summarized as below:

(i) The optimized geometries show that the global minimum structures of S_n^Q (n = 3-20, Q = 0, ±1) clusters prefer closed 3D helical ring forms. The ground state structures of cationic sulfur clusters are similar to those of neutral species except for n = 7, 13, 14, 17 and 20. However, the equilibrium structures of anionic sulfur are clearly distinguished from the neutral and cationic geometries.

(ii) The calculated average binding energies, second-order energy differences and HOMO–LUMO gaps results have indicated that the neutral S_8 and S_{12}, as well as cationic S_5^+ and S_{14}^+, possess enhanced relative stability.

(iii) According to the fragmentation energy E_f, it is found that the $S_n^Q \rightarrow S_2 + S_{n-2}^Q$ channel is a route that the small clusters (n = 3-10) favor, while the larger clusters (n = 13-20) prefer the $S_n^Q \rightarrow S_8 + S_{n-8}^Q$ channel. In addition, the E_f vs. n curves suggests that the clusters with larger size are relatively more unstable and easier dissociated.

(iv) The calculated ionization energies and electron affinity are in good agreement with the experimental determinations. Further detailed investigations on sulfur clusters are needed in order to clarify various important aspects of size effects on the stability and electronic properties.

Acknowledgements

This work was supported by the National Natural Science Foundation of China (Nos. 11304167 and 11274235), Postdoctoral Science Foundation of China (Nos. 20110491317 and 2014T70280), Program for Science & Technology Innovation Talents in Universities of Henan Province (No. 15HASTIT020), Open Project of State Key Laboratory of Superhard Materials (No. 201405), and Young Core Instructor Foundation of Henan Province (No. 2012GGJS-152).

Notes and references

[a] Institute of Atomic and Molecular Physics, Sichuan University, Chengdu 610065, China.

[b] Department of Chemistry, University of Patras, GR-26500 Patras, Greece.

[c] Department of Physics, Nanyang Normal University, Nanyang 473061, China.

[d] State Key Laboratory of Superhard Materials, Jilin University, Changchun 130012, China.

[e] Beijing Computational Science Research Center, Beijing 100084, China.

Electronic mail: scu_kuang@163.com, lucheng@calypso.cn, lvjian@calypso.cn.

† Electronic Supplementary Information (ESI) available: [details of the low-lying isomers, vibrational frequencies, HOMO-LUMO energy

gaps and cartesian coordinates of neutral and charged sulfur clusters]. See DOI: 10.1039/b000000x/

1 C. Chen, T. Wang, S. Varadharaj, L. A. Reyes, C. Hemann, M. A. H. Talukder, Y. Chen, L. J. Druhan and J. L. Zweier, Nature, 2010, **468**, 1115.
2 A. C. McQuilken and D. P. Goldberg, Dalton Trans., 2012, **41**, 10883.
3 O. Stehling, A. A. Vashisht, J. Mascarenhas, Z. O. Jonsson, T. Sharma, D. J. A. Netz, A. J. Pierik, J. A. Wohlschlegel and R. Lill, Science, 2012, **337**, 195.
4 K. Hou and W. Y. Fan, Dalton Trans., 2014, **43**, 16977.
5 E. Miliordos and S. S. Xantheas, J. Am. Chem. Soc., 2014, **136**, 2808.
6 L. Chen, X. Cui, Y. Wang, M. Wang, R. Qiu, Z. Shu, L. Zhang, Z. Hua, F. Cui, C. Wei and J. Shi, Dalton Trans., 2014, **43**, 3420.
7 G. Liu, P. Niu, L. Yin and H. M. Cheng, J. Am. Chem. Soc., 2012, **134**, 9070.
8 O. Degtyareva, E. Gregoryanz, M. Somayazulu, P. Dera, H. K. Mao and R. J. Hemley, Nat. Mater., 2005, **4**, 152.
9 R. Steudel, in *Studies in Inorganic Chemistry*, edited by A. Miiller and B. Krebs (Elsevier, Amsterdam. 1984), Vol. **5**, p. 3 and references therein.
10 S. Hunsicker, R. O. Jones and G. Ganteför, J. Chem. Phys., 1995, **102**, 5917.
11 R. Bellissent, L. Descotes, F. Bou é and P. Pfeuty, Phys. Rev. B, 1990, **41**, 2135.
12 A. G. Kalampounias, K. S. Andrikopoulos and S. N. Yannopoulos, J. Chem. Phys., 2003, **118**, 8460.
13 T. P. Martin, J. Chem. Phys., 1984, **81**, 4426.
14 D. Hohl, R. O. Jones, R. Car and M. Parrinello, J. Chem. Phys., 1988, **89**, 6823.
15 K. Raghavachari, C. M. Rohlfing and J. S. Binkley, J. Chem. Phys., 1990, **93**, 5862.
16 S. Millefiori and A. Alparone, J. Phys. Chem. A, 2001, **105,** 9489.
17 R. O. Jones and P. Ballone, J. Chem. Phys., 2003, **118**, 9257.
18 Y. C. Wang, J. Lv, L. Zhu and Y. M. Ma, Phys. Rev. B, 2010, **82,** 094116.
19 Y. C. Wang, J. Lv, L. Zhu and Y. M. Ma, Comput. Phys. Commun., 2012, **183,** 2063.
20 Y. C. Wang, M. S. Miao, J. Lv, L. Zhu, K. T. Yin, H. Y. Liu, and Y. M. Ma, J. Chem. Phys., 2012, **137**, 224108.
21 L. Zhu, H. Y. Liu, C. J. Pickard, G. T. Zou and Y. M. Ma, Nature Chem. 2014, **6**, 644.
22 S. H. Lu, Y. C. Wang, H. Y. Liu, M. S. Miao and Y. M. Ma, Nature. Commun., 2014, **5**, 3666.
23 A. D. Becke, J. Chem. Phys., 1993, **98**, 5648.
24 J. P. Perdew and Y. Wang, Phys. Rev. B, 1992, **45**, 13244.
25 *Electronic Structure of Solids*, edited by J. P. Perdew, P. Ziesche and H. Eschrig, Akademie Verlag, Berlin, 1991.
26 M. J. Frisch, G. W. Trucks, H. B. Schlegel, G. E. Scuseria, M. A. Robb, J. R. Cheeseman, J. A. Montgomery Jr, T. Vreven, K. N. Kudin, J. C. Burant, J. M. Millam, S. S. Iyengar, J. Tomasi, V. Barone, B. Mennucci, M. Cossi, G. Scalmani, N. Rega, G. A. Petersson, H. Nakatsuji, M. Hada, M. Ehara, K. Toyota, R. Fukuda, J. Hasegawa, M. Ishida, T. Nakajima, Y. Honda, O. Kitao, H. Nakai, M. Klene, X. Li, J. E. Knox, H. P. Hratchian, J. B. Cross, V. Bakken, C. Adamo, J. Jaramillo, R. Gomperts, R. E. Stratmann, O. Yazyev, A. J. Austin, R. Cammi, C. Pomelli, J. Ochterski, P. Y. Ayala, K. Morokuma, G. A. Voth, P. Salvador, J. J. Dannenberg, V. G. Zakrzewski, S. Dapprich, A. D. Daniels, M. C. Strain, O. Farkas, D. K. Malick, A. D. Rabuck, K. Raghavachari, J. B. Foresman, J. V. Ortiz, Q. Cui, A. G. Baboul, S. Clifford, J. Cioslowski, B. B. Stefanov, G. Liu, A. Liashenko, P. Piskorz, I. Komaromi, R. L. Martin, D. J. Fox, T. Keith, M. A. Al-Laham, C. Y. Peng, A. Nanayakkara, M. Challacombe, P. M. W. Gill, B. G. Johnson, W. Chen, M. W. Wong, C. Gonzalez and J. A. Pople, Gaussian 09 Revision C.0, Gaussian, Inc., Wallingford, CT, 2009.
27 D. A. Dixon and E. Wasserman, J. Phys. Chem., 1990, **94**, 5112.
28 R. Steudel, J. Steidel and T. Sandow, Z. Naturforsch. Teil B, 1986, **41**, 958.
29 M. D. Chen, M. L. Liu, L. S. Zheng, Q. E. Zhang and C. T. Au, Chem. Phys. Lett., 2001, **350**, 119.
30 V. G. Zakrzcwski and W. Niessen, Theor. Chim. Acta, 1994, **88**, 75.
31 M. D. Chen, M. L. Liu, J. W. Liu, Q. E. Zhang and C. T. Au, J. Mol. Struct. (theochem), 2002, **582**, 205.
32 V. M. Medel, A. C. Reber, V. Chauhan, P. Sen, A. M. Köster, P. Calaminici and S. N. Khanna, J. Am. Chem. Soc., 2014, **136**, 8229.
33 N. Akman, M. Tas, C. Özdoğan and I. Boustani, Phys. Rev. B, 2011, **84**, 075463.
34 J. Berkowitz and C. Lifshitz, J. Chem. Phys., 1968, **48**, 4346.
35 H. M. Rosenstock, K. Draxel, B. W. Steiner and J.T. Herron, *Energetics of Gaseous Ions*, J. Phys. Chem. Ref. Data **6**, Suppl.1 (1977).